GC Base Sequence Recognition by Oligo(imidazolecarboxamide) and C-Terminus-Modified Analogues of Distamycin Deduced from Circular Dichroism, Proton Nuclear Magnetic Resonance, and Methidiumpropylethylenediaminetetraacetate–Iron(II) Footprinting Studies

Moses Lee,*,‡ Andrea L. Rhodes,‡ Michael D. Wyatt,‡ Stephen Forrow,§ and John A. Hartley§

Department of Chemistry, Furman University, Greenville, South Carolina 29613, and Department of Oncology, University College and Middlesex School of Medicine, London, U.K. W1P 8BT

Received September 9, 1992; Revised Manuscript Received February 16, 1993

ABSTRACT: The DNA binding properties of a series of imidazole-containing and C-terminus-modified analogues **4**–**7** of distamycin are described. These analogues contain one to four imidazole units, respectively. Data from the ethidium displacement assay showed that these compounds bind in the minor groove of DNA, with the relative order of binding constants of **6** (Im_3) > **7** (Im_4) > **5** (Im_2) > **4** (Im_1). The reduced binding constants of these compounds for poly(dA–dT) relative to distamycin, while they still interact strongly with poly(dG-dC), provided evidence of GC sequence acceptance. The preferences for GC-rich sequences by these compounds were established from a combination of circular dichroism (CD) titration, proton nuclear magnetic resonance (^{1}H-NMR), and methidiumpropylethylenediaminetetraacetate–iron(II) [MPE·Fe(II)] footprinting studies. In the CD studies, these compounds produced significantly larger DNA-induced ligand bands with poly(dG-dC) than poly(dA-dT) at comparable ligand concentrations. ^{1}H-NMR studies of the binding of **5** to d-[CATGGCCATG]$_2$ provided further evidence of the recognition of GC sequences by these compounds, and suggested that the ligand was located on the underlined sequence in the minor groove with the C-terminus oriented over the T residue. MPE footprinting studies on a GC-rich *Bam*HI/*Sal*I fragment of pBR322 provided unambiguous evidence for the GC sequence selectivity for some of these compounds. Compounds **4** and **7** produced poor footprints on the gels; however, analogues **5** and **6** gave strong footprints. Detailed densitometric analyses of the gels showed that the preferred binding sites of **5** was at 5′-(G·C)$_3$(A·T), i.e., three GC based pairs followed by an AT base pair, whereas the strongest footprint sites for **6** were within two occurrences of the sequence 5′-TCGGGCT. These results also showed that **5** and **6** bind to different sequences on the same DNA fragment, even though they differ by only one imidazole unit. Molecular modeling experiments were performed to rationalize the lower binding affinity of tetraimidazole analogue **7** compared to triimidazole **6**. The radius of curvature of **7** (13 ± 1 Å) was found to be higher than the other compounds (15 ± 1 and 17 ± 1 Å for **5** and **6**, respectively), and this presumably hinders its interaction with the convex surface of the B-DNA conformation of d-[G_4·C_4], which has a curvature of 19 ± 1 Å.

There is currently interest in the development of low molecular weight, sequence-specific DNA binding agents for chemotherapy (Caruthers, 1980; Frederick et al., 1984; Gurskii, 1977; Hurley, 1989; Lown, 1988; Takeda et al., 1983; Watson et al., 1987), for use as structural (Barton, 1986) and gene (Bains, 1989) probes, and as artificial restriction enzymes (Mark et al., 1988; Helene, 1990). One goal in this type of DNA research is to develop molecules that can recognize specific DNA sequences, with the intention of modifying gene expression (Krowicki et al., 1988; Watson et al., 1987). There is particular interest in developing ligands with GC base sequence selectivity because most of the known DNA minor-groove binding compounds are AT-sequence-specific. This interest also stems from the observation that regions of high GC content are commonly found in genomes of mammals, including humans, and that a functional role of GC-rich sequences is suggested by their frequent occurrence in genes associated with proliferation, including a number of oncogenes (Mattes et al., 1988; Hartley et al., 1988).

Minor-groove binding agents are attractive for the development of DNA sequence-selective compounds because there are precedents for such interactions (Krowicki et al., 1988; Zimmer, 1986; Dervan, 1986). It has been shown that imidazole-containing analogues of netropsin (**1**) and distamycin (**2**) (see Figure 1) have increased selectivity for GC-rich sequences. For example, DNAse I footprinting studies of the monocationic bisimidazole ligand **3** showed that it not only recognized GC base pairs but also reads the 5′-CCGT-3′ sequence (Kissinger et al., 1987). NMR[1] and X-ray studies provided an explanation for the reading of a 3′-terminal AT base pair (Lee et al., 1987).

If the human genome is the target for a uniquely sequence-selective agent, the distinguishable sequence would have a binding site size of 15–16 base pairs (Dervan, 1986). As the AT-sequence-selective distamycin analogues increased in length, the hydrogen bond and van der Waals contacts between the ligand and DNA become seriously "out of phase" with the

‡ Furman University.
§ University College and Middlesex School of Medicine.

[1] MPE, methidiumpropylethylenediaminetetraacetate; CD, circular dichroism; IR, infrared; UV–vis, ultraviolet–visible; FAB-MS, fast atom bombardment mass spectrometry; HRMS, high-resolution mass spectrometry; EI, electron ionization; ^{1}H-NMR, proton nuclear magnetic resonance; TLC, thin-layer chromatography; NOE, nuclear Overhauser effects; EtBr, ethidium bromide; HDO, hydrogen deuterium oxide; DMSO, dimethyl sulfoxide; DTT, dithiothreitol; EDTA, ethylenediaminetetraacetic acid; TFA, trifluoroacetic acid; NBA, *n*-butylamine.

0006-2960/93/0432-4237$04.00/0

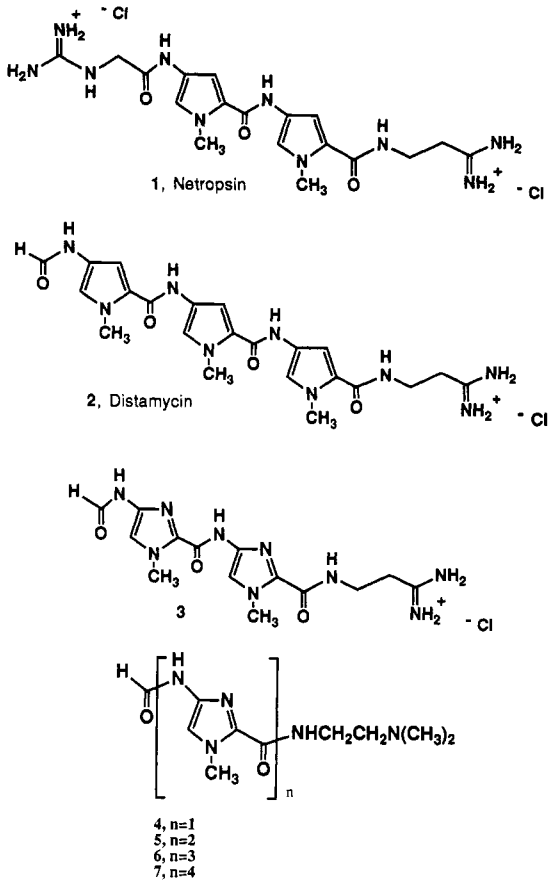

FIGURE 1: Structures of the compounds studied.

spacing between the nucleotide units of DNA (Goodsell & Dickerson, 1986; Lown, 1988). This phenomenon may explain the reduced binding affinities exhibited by oligo(*N*-methylpyrrole) peptides (Younguist & Dervan, 1985a,b; Luck et al., 1977). There is an optimum number of heterocyclic moieties which these compounds can have and still bind to DNA effectively. Therefore, in our studies toward the development of ligands that can recognize long GC-rich sequences, we report herein the DNA sequence binding selectivities of a series of oligo(imidazolecarboxamide) analogues **4**–**7** (see Figure 1) of distamycin deduced from ^{1}H-NMR, MPE footprinting, and CD as well as molecular modeling studies. In these analogues the C-terminus has a dimethylaminoethyl group instead of the amidine present in distamycin (Lee et al., 1992). The dimethylamino moiety has been found to behave similarly to the amidine moiety with respect to DNA sequence selectivity (Taylor et al., 1984).

MATERIALS AND METHODS

The ^{1}H-NMR spectra were recorded on a Varian VXR 300S spectrometer, and the resonance positions are reported in parts per million from the HDO or the TMS signal. Fluorescence assays were performed on an Aminco-Bowman spectrophotofluorometer. UV–vis spectra were obtained on a Hewlett-Packard 8452A diode array spectrophotometer. DNA synthesis was performed on an Applied Biosystems 391 DNA synthesizer, PCR-Mate, and purified by ethanol precipitation. Biochemicals (DNA) were purchased from Pharmacia.

N-[2-(Dimethylamino)ethyl]-4-formamido-1-methylimidazole-2-carboxamide (**4**). Acetic formic anhydride was prepared by cooling dry acetic anhydride (6 mL) to 0 °C, slowly adding dry formic acid (3 mL), heating at 50 °C for 15 min, and cooling immediately to 0 °C.

A solution of *N*-[2-(dimethylamino)ethyl]-1-methyl-4-nitroimidazole-2-carboxamide (302 mg, 1.25 mmol) in methanol (50 mL) was hydrogenated over 5% Pd on carbon (115 mg) at room temperature and atmospheric pressure until TLC analysis indicated complete reduction of the starting material (2.5 h). The catalyst was removed by filtration. The filtrate was concentrated, and the residue was coevaporated with dry CH_2Cl_2 (20 mL, twice) to give 4-amino-*N*-[2-(dimethylamino)ethyl]-1-methylimidazole-2-carboxamide as a yellow oil, which was unstable and thus used directly in the next step.

A solution of the above amine in dry CH_2Cl_2 (40 mL) was added dropwise to the cooled and stirred solution of acetic formic anhydride under a drying tube. The suspension was allowed to warm to room temperature and stirred overnight (17 h), at which time a clear yellow solution was obtained. After TLC analysis indicated all of the starting material was gone, the reaction mixture was cooled to 0 °C for 15 min and quenched with the addition of methanol (50 mL). The reaction mixture was concentrated under reduced pressure and coevaporated with additional methanol (50 mL, twice). The yellow oily residue was dissolved in CH_2Cl_2 (100 mL) and washed sequentially with saturated $NaHCO_3$ (100 mL) and water (100 mL). The organic layer was dried (Na_2SO_4) and concentrated to a yellow oil. To the combined aqueous layers were added 10% NH_4OH (to make the pH > 7) and NaCl (2 g); the mixture was then extracted with $CHCl_3$ (100 mL, five times). The organic layers were combined, dried (Na_2SO_4), and concentrated to a yellow oil which was purified by column chromatography (silica gel) with 5% methanol in chloroform as eluent. The desired fractions were combined and concentrated to an oily residue which was then converted to its hydrochloride salt by dissolving the oil in ether (30 mL) and bubbling with dry HCl gas. The off-white solid was collected and dried in vacuo at room temperature. Yield 233 mg (0.974 mmol, 78%): mp 149 °C (decompn); TLC (10% MeOH/$CHCl_3$) R_f 0.04; IR ($CHCl_3$) ν 3422, 3019, 1668, 1571, 1537, 1214, and 748 cm^{-1}; ^{1}H-NMR ($CDCl_3$) δ 2.17 (s, 6 H, NMe_2) 2.42 (t, J = 5.5 Hz, 2 H, CH_2NMe_2), 3.36 (q, J = 5.5 Hz, 2 H, NCH_2C), 3.86 (s, 3 H, imidazole 1-Me), 7.27 (s, 1 H, imidazole), 7.72 (br s, 1 H, NH), 8.20 (s, 1 H, formyl), and 10.05 (s, 1 H, NH); MS (FAB-glycerin) m/e (relative intensity) 240 ($M-Cl^-$, 45). HRMS (FAB-glycerin) Calcd for $C_{10}H_{18}N_5O_2$: 240.1732. Found: 240.1730.

N-[2-(Dimethylamino)ethyl]-4-[4-formamido-1-methylimidazole-2-carboxamido]-1-methylimidazole-2-carboxamide (**5**). The procedure is similar to that for the synthesis of **4**, except compound *N*-[2-(dimethylamino)ethyl]-4-[1-methyl-4-nitroimidazole-2-carboxamido]-1-methylimidazole-2-carboxamide was used. The product **5**, as the free amine, was isolated as an off-white powder. Yield 207 mg (0.57 mmol, 42%): mp 133 °C (decompn); TLC (10% MeOH/$CHCl_3$) R_f 0.08; IR (Nujol) ν 3400, 2700, 1654, 1540, and 668 cm^{-1}; ^{1}H-NMR ($CDCl_3$) δ 2.27 (s, 6 H, NMe_2), 2.45 (t, J = 6.0 Hz, 2 H, CH_2NMe_2), 3.50 (q, J = 6.0 Hz, 2 H, NCH_2C), 3.95 (s, 3 H, imidazole 1-Me), 4.05 (s, 3 H, imidazole 1-Me), 7.35 (s, 1 H, imidazole), 7.45 (s, 1 H, imidazole), 8.10 (br s, 1 H, NH), 8.35 (s, 1 H, formyl), 9.40 (br s, 1 H, NH), and 9.60 (s, 1 H, NH); ^{13}C-NMR ($CDCl_3$) δ 35.3, 36.6, 45.2, 58.1, 113.0, 115.1, 135.7, 135.0, 135.3, 1155.7, 157.9, and 259.4; UV (water) λ_{max} 202 ($\epsilon = 3.5 \times 10^4$ cm^{-1} M^{-1}), 214 ($\epsilon = 3.7 \times 10^4$ cm^{-1} M^{-1}), and 302 nm ($\epsilon = 1.1 \times 10^4$ cm^{-1} M^{-1}); MS (EI) m/e (relative intensity) 362 (M^+, 6), 292 (13), 148 (9); HRMS (EI) Calcd for $C_{15}H_{22}N_8O_3$: 362.1814. Found: 362.1812.

N-[2-(*Dimethylamino*)*ethyl*]-*1-methyl-4*-{*1-methyl-4*-[*4-formamido-1-methylimidazole-2-carboxamido*]*imidazole-2-carboxamido*}*imidazole-2-carboxamide* (**6**). The procedure is similar to that for the synthesis of **4**, except compound *N*-[2-(dimethylamino)ethyl]-1-methyl-4-{1-methyl-4-[1-methyl-4-nitroimidazole-2-carboxamido]imidazole-2-carboxamido}-imidazole-2-carboxamide was used. The product **6**, as the free amine, was isolated as an off-white powder. Yield 212.2 mg (0.438 mmol, 56%): mp 239–242 °C; TLC (10% MeOH/$CHCl_3$) R_f 0.11; IR (Nujol) ν 3384, 1676, 1542, 1121, and 905 cm^{-1}; ^{1}H-NMR ($CDCl_3$) δ 2.28 (s, 6 H, NMe_2), 2.47 (t, J = 5.5 Hz, 2 H, CH_2NMe_2), 3.48 (q, J = 5.5 Hz, 2 H, NCH_2C), 4.00 (s, 3 H, imidazole 1-Me), 4.05 (s, 6 H, imidazole 1-Me) 7.35 (s, 1 H, imidazole), 7.43 (s, 1 H, imidazole), 7.47 (s, 1 H, imidazole), 7.64 (br t, J = 5.5 Hz, 1 H, NH), 8.35 (s, 1 H, formyl), 8.40 (s, 1 H, NH), 9.43 (br s, 1 H, NH), and 9.50 (br s, 1 H, NH); ^{13}C-NMR ($CDCl_3$) δ 35.6, 36.6, 45.3, 58.2, 102.0, 115.1, 123.0, 135.1, 135.5, 155.7, 155.8, and 158.0; UV (water) λ_{max} 214 ($\epsilon = 5.5 \times 10^4$ cm^{-1} M^{-1}) and 304 nm ($\epsilon = 2.4 \times 10^4$ cm^{-1} M^{-1}); MS (FAB, TFA-NBA) m/e (relative intensity) 486 (M + H^+, 100). Anal. Calcd for $C_{20}H_{27}N_{11}O_4.1/2H_2O$: C, 48.57; H, 5.72. Found: C, 48.96; H, 6.15.

N-[2-(*Dimethylamino*)*ethyl*]-*1-methyl-4*-{*1-methyl-4*-[*1-methyl-4*-(*4-formamido-1-methylimidazole-2-carboxamido*)-*imidazole-2-carboxamido*]*imidazole-2-carboxamido*}-*imidazole-2*-carboxamide (**7**). The procedure is similar to that for the synthesis of **4**, except compound *N*-[2-(dimethylamino)ethyl]-1-methyl-4-{1-methyl-4-[1-methyl-4-(1-methyl-4-nitroimidazole-2-carboxamido)-imidazole-2-carboxamido]-imidazole-2-carboxamido}-imidazole-2-carboxamide was used. The product **7**, as the free amime, was isolated as an off-white solid. Yield 21.5 mg (0.0354 mmol, 12%): mp 162–176 °C (decompn); TLC (10% MeOH/$CHCl_3$) R_f 0.07; IR ($CHCl_3$) ν 3384, 2923, 1654, and 1540 cm^{-1}; ^{1}H-NMR ($CDCl_3$) δ 2.28 (s, 6 H, NMe_2), 2.41 (t, J = 5.5 Hz, 2 H, CH_2NMe_2), 3.35 (q, J = 5.5 Hz, 2 H, NCH_2C), 4.02 (s, 12 H, imidazole 1-Me), 7.31 (s, 1 H, imidazole), 7.38 (s, 1 H, imidazole), 7.40 (s, 1 H, imidazole), 7.45 (s, 1 H, imidazole), 7.75 (br s, 1 H, NH), 8.27 (s, 1 H, formyl), 9.43 (br s, 1 H, NH), 9.58 (br s, 1 H, NH), 9.75 (br s, 1 H, NH), 9.85 (br s, 1 H, NH); MS (FAB, NBA) m/e (relative intensity) 609 (M + H^+, 6); HRMS (FAB, NBA) Calcd for $C_{25}H_{32}N_{14}O_5H$: 609.2741. Found: 609.2758.

MPE Footprinting. pBR322 plasmid DNA was obtained from Northumbria Biologicals Ltd. Sonicated calf thymus DNA was from Pharmacia and was dissolved to 1 mg/mL in 10 mM Tris, pH 7.4, and 50 mM NaCl and stored at −20 °C. Formic acid was purchased from Sigma, Poole, Dorset, England. MPE was a generous gift from Professor P. B. Dervan, California Institute of Technology. The solutions of compounds **4**–**7** were prepared fresh immediately before use or used from frozen stock solutions. In either case the ligands were made up in DMSO and 1 equiv of HCl.

All footprinting experiments were carried out on either the *Hin*dIII/*Eco*RI or *Bam*HI/*Sal*I restriction fragment of pBR322 DNA. The linearized DNA was 5′-end-labeled at either the *Sal*I or the *Bam*HI site using [γ-^{32}P]ATP and T4 polynucleotide kinase under standard conditions, the reaction products were separated using a Prep-Gel (Bio-Rad) preparative electrophoresis apparatus system, and the required fragments were concentrated by lyophilization. The DNA was washed twice with 70% ethanol and dried before being dissolved in 10 mM Tris, pH 7.4, and 50 mM NaCl.

Table I: Association Constants ($K_{app} \times 10^5$ M^{-1}) of Compounds with Polynucleotides

compd	calf thymus DNA	T4 DNA	poly(dA-dT)	poly(dG-dC)
EtBr	100[a]	100[b]	95[b]	99[b]
2[c]	7.7	6.5	348	2.0
4	0.3 ± 0.2			0.02 ± 0.01
5	0.3 ± 0.2	0.4 ± 0.2	0.2 ± 0.2	0.2 ± 0.2
6[c]	7.7	6.7	5.9	6.1
7[c]	3.4	3.3	4.8	5.3

[a] Morgan et al. (1979). [b] Debart et al. (1989). [c] The error for compounds **2**, **6**, and **7** is $\pm 0.1 \times 10^5$ M^{-1}.

MPE footprinting was carried out by combining the singly end-labeled pBR322 restriction fragments, sonicated calf thymus DNA, and the drug in buffer (10 mM Tris, pH 7.4, and 50 mM NaCl). After incubation for 2 h at room temperature, MPE·Fe(II), from a freshly prepared mixture of $Fe(NH_4)_2(SO_4)2{\cdot}6H_2O$ and MPE, followed by DTT, was added to each reaction. The final solutions contained 150 μM base pairs DNA, 10 mM MPE·Fe(II), 2 mM DTT, and drug (100, 250, and 500 μM) in a total volume of 38 μL. Cleavage reactions were left for 25 min at room temperature and were stopped by snap-freezing at −78 °C. The solutions were then lyophilized and resuspended in formamide loading buffer. Electrophoresis of the samples was performed on sequencing gels (0.4 mm thick × 80 cm long, 8% polyacrylamide and 7 M urea, 3000 V, 60 °C). The gels were dried (Bio-Rad Model 583 slab-gel dryer) and autoradiographed at −70 °C using Amersham Hyperfilm MP. The resulting autoradiograms were scanned using a LKB Ultrascan laser-enhanced densitometer.

Ethidium Displacement Assay. To 2 mL of ethidium bromide buffer, pH 7.4, was added 25 μL of DNA solution (A_{260nm} = 2), and the maximum fluorescence was measured (excitation wavelength = 546 nm, emission wavelength = 600 nm) at room temperature. Aliquots of a 10 mM stock drug solution (1 mg of drug to be tested and the appropriate volume of distilled water to make a 10 mM solution) were then added to the DNA–ethidium solution, and the fluorescence was measured after each addition until a 50% reduction of fluorescence had occurred. If the 10 mM stock solution lowered the percent fluorescence too quickly, the solution was further diluted to 1 mM prior to titration. The apparent binding constant was calculated from

$$K_{EtBr}[EtBr] = K_{app}[drug]$$

where [drug] = the concentration of drug at a 50% reduction of fluorescence and K_{EtBr} (see Table I) and [EtBr] are known. The concentration of ethidium bromide was 1.3 μM.

CD Titration Studies. All experiments were performed with a continuous flow of nitrogen purging the polarimeter. A 1-mm path length jacketed cell was used and all experiments were done at room temperature. Initially, DNA [154 μM (bp), 130 μL] was placed in the cell and the spectrum of the DNA alone was reported. Aliquots of drug were then added and each of the spectra was reported. The aqueous drug solutions (as the hydrochloride salt) were 1 mM, and amounts of the drug added corresponded to the moles of drug: moles of DNA base pairs ratios (r') of 0.02, 0.10, 0.15, 0.20, 0.25, 0.30, 0.35, 0.40, 0.50, 0.60, 0.80, and 1.00.

The scan parameters were set were as follows: The spectra collected were from 400 to 220 nm, and the sensitivity was set at 1 mdeg with a scan speed of 200 nm/min. Three scans were accumulated and automatically averaged by the computer. The λ_{max} and ellipticity (millidegrees) for each spectrum

were collected from the raw scans and the final plots were smoothed by the noise reduction program, which uses a low-pass digital filter on the computer.

Sample Preparation and NMR Spectroscopy. The sample of the decadeoxyribonculeotide was prepared by dissolving 12.2 mg of the oligomer in a 99.8% D_2O solution (Aldrich) containing 30 mM potassium phosphate buffer (pH 7.0), 0.01 mM EDTA, and 10 mM NaCl. The solution was lyophilized twice with 99.8% D_2O and once with 99.996% D_2O (Aldrich), and finally made up to 0.35 mL with 99.996% D_2O. A fresh solution of **5**, 44 mM in 50 mL of 4% DMSO-d_6 in 99.996% D_2O, was prepared just before the experiment. NMR spectra were obtained at 25 or 37 °C.

Two-dimensional spectra were recorded with magnitude detection. Phase-sensitive NOESY spectra with mixing times of 0.1 and 0.4 s were recorded with 1024 data points in the t_2 dimension, 128 transients per t_1 increment, and 128 increments in the t_1 dimension with zero-filling to 1024 data points. Absolute COSY experiments were recorded using the RELAYH program with 128 increments in the t_1 dimension wiht zero-filling to 1024 data points. The acquisition time was 0.212 s, pulse width was 17 μs (90°), sweep width was 2411 Hz, and relaxation delay was 3 s.

Molecular Modeling. The DNA structures were drawn using DNA/RNA builder (Atlantic Software) and modeled on the Tektronix CAChe system. The structures of the ligands were energy-minimized using MM2 parameters and constrained to 0.1 kcal mol^{-1}.

RESULTS AND DISCUSSION

DNA Sequence and Groove Binding Selectivity. The apparent DNA binding constants (K_{app}) of the four imidazole-containing analogues **4**–**7** (see Figure 1) to calf thymus DNA, T4 coliphage DNA, poly(dA-dT), and poly(dG-dC) were determined using the ethidium displacement assay (Morgan et al., 1979; Debart et al., 1989) and were compared to those of distamycin (see Table I). These data demonstrate that all compounds can bind to the DNAs studied. The values of K_{app} for **4** and **5** are lower than those of distamycin. This lower affinity could be due to the lower number of amide moieties in **4** and **5** (two and three, respectively, versus four), and van der Waals contacts compared to distamycin. The K_{app} values of the tri- and tetraimidazole analogues **6** and **7** are comparable to the parent distamycin for calf thymus and T4 coliphage DNA. However, a number of differences were observed in their binding properties to poly(dA-dT) and poly(dG-dC). Compounds **6** and **7** bind significantly more weakly to poly(dA-dT) but slightly more strongly to poly(dG-dC) than distamycin, suggesting that these analogues can accept GC base pairs. The values of K_{app} of poly(dG-dC) for **5** and **6** are slightly greater than those for poly(dA-dT), while the K_{app} of poly(dG-dC) for distamycin is about 2 orders of magnitude lower than the K_{app} of poly(dA-dT). These results agree with the proposal that changing the pyrrole moieties in distamycin to imidazole groups increases the acceptance of these compounds for GC base pairs and implies that the concave imidazole–nitrogen atom could accept a hydrogen bond from the guanine 2-amino moiety. It is worthy to note that the values of K_{app} for the tetraimidazole **7** are lower than those of the triimidazole analogue **6**, suggesting that the optimum number of heterocyclic units of these compounds for binding to the DNA could be three.

The large apparent binding constants (comparable to those of distamycin) for T4 coliphage DNA for compounds **6** and **7** gave evidence of their minor-groove selectivity, because the major groove of T4 coliphage DNA is blocked by α-glycosylation of the 5-(hydroxymethyl)cytidine residues (Lown, 1982). These results are in agreement with the binding of distamycin to the minor groove of d-$[CGCAAATTTGCG]_2$, as shown by an X-ray crystallography study (Coll et al., 1987).

Circular Dichroism Studies. The conformation of DNA can be readily determined by CD experiments, and for B-DNA, characteristic positive and negative Cotton effects are observed at 260 and 245 nm, respectively (see Figure 2A). The interactions of the oligoimidazole analogues **4**–**7** with poly(dG-dC), poly(dA-dT), and calf thymus DNA were monitored by CD measurements similar to those previously reported for the nonintercalators netropsin and the imidazole-containing lexitropsins (Burckhardt et al., 1989; Zimmer, 1986; Zimmer et al., 1988).

No changes in the CD spectra were observed upon titration of the monoimidazole analogue **4** with poly(dG-dC) or poly(dA-dT), thereby suggesting that the ligand has minimal interaction with the DNAs. These results are consistent with the low K_{app} of this compound for poly(dG-dC). Further results show that compounds **5**–**7** bind to the DNAs studied as indicated by the appearance of DNA-induced ligand CD bands at about 300–340 nm, presumably due to the UV absorption π to π^* transition of the drug in the drug·DNA complex. The appearance of a DNA-induced ligand CD band is clear evidence of the interactions of the molecules with the DNA because these compounds do not exhibit any CD spectra by themselves. Representative CD spectra for compound **6** with the above DNAs are shown in Figure 2. Titration of the triimidazole analogue **6** to poly(dA-dT) produced a negative Cotton effect at 308 nm (1.2 mdeg at $r' = 0.6$) (see Figure 2A). However, titration of **6** to poly(dG-dC) gave rise to a significantly more intense positive Cotton effect band at 332 nm (1.8 mdeg, $r' = 0.25$), and a negative band at 300 nm (1.5 mdeg, $r' = 0.25$) (see Figure 2B). Addition of compound **6** to calf thymus DNA at drug concentrations $r' < 0.6$ also produced a strong positive band at 332 nm (5 mdeg, $r' = 0.2$), a negative band at 300 nm (1.5 mdeg, $r' = 0.2$) (see Figure 2C). The largest ligand-induced CD bands of **5**–**7** at these wavelengths occur with calf thymus DNA (42% GC) and poly(dG-dC). Under similar conditions and comparable r' (moles of added ligand to moles of DNA base pairs), these compounds produced weaker induced bands with poly(dA-dT). These data suggest that the oligoimidazole analogues have more affinity for GC-rich sequences than distamycin (Burckhardt et al., 1989; Zimmer, 1986; Zimmer et al., 1988).

In the above CD experiments, the presence of the negative and positive bands of the DNA at ~245 and ~270 nm, respectively, suggest that the conformation of the DNA in the ligand·DNA complexes remained in the B-form (see Figure 2). In order to further investigate the structural requirements for the interactions of these analogues with DNA, a ^{1}H-NMR study on the 1:1 complex of **5** with the decadeoxyribonucleotide d-$[CATGGCCATG]_2$ was undertaken.

*Titration and Binding of **5** to d-$[C_1A_2T_3G_4G_5C_6C_7A_8T_9G_{10}]_2$.* The results of the titration of **5** into the decadeoxyribonucleotide are shown in Figure 3B–D, together with the partially assigned reference spectrum of the free DNA (Figure 3A) (Lee et al., 1987). These studies were performed using procedures similar to those previously reported for the binding of **3** to the same decamer (Lee et al., 1987). With increasing proportions of **5** the ^{1}H-NMR resonances of the decamer showed distortion of the line shapes resulting from signal broadening, presumably due to chemical exchange occurring on the NMR time scale and/or the increased correlation time

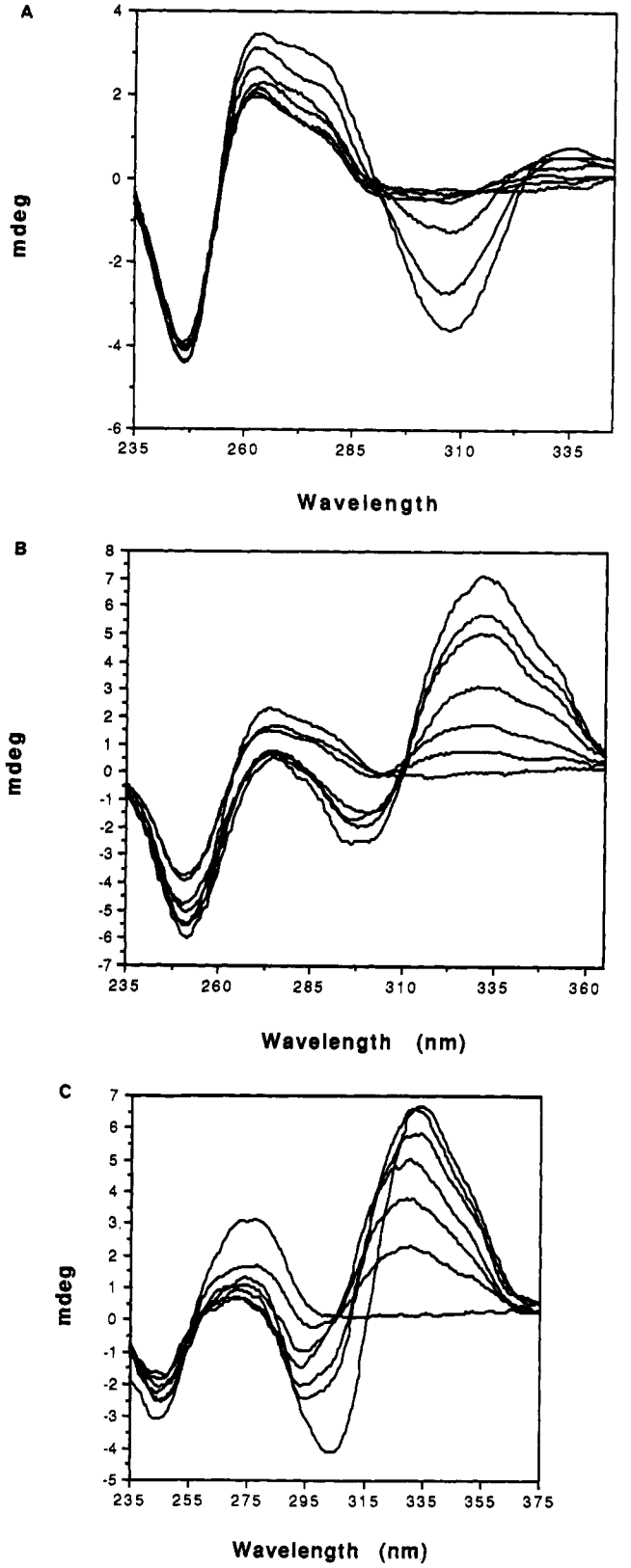

FIGURE 2: CD titration of the triimidazole analogue **6** into (A) poly-(dA-dT), (B) poly(dG-dC), and (C) calf thymus DNA. The plots correspond to r' values of 0, 0.05, 0.10, 0.20, 0.40, 0.60, 0.80, and 1.0 for poly(dA-dT) and calf thymus DNA. For poly(dG-dC), the r' values are 0, 0.12, 0.25, 0.35, 0.5, and 0.6. The r' values are defined as the input ratio of the moles of ligand to DNA base pairs.

(James, 1975), and ligand-induced chemical shift changes. In addition, some new resonances appeared which increased in proportion to the amount of drug added (Figure 3B,C), thus

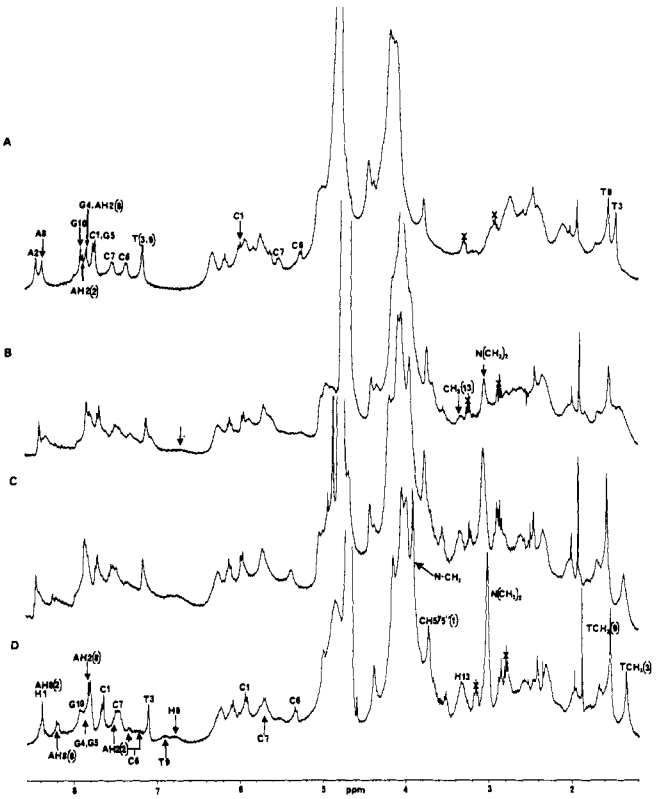

FIGURE 3: NMR titration of d-[CATGGCCATG]$_2$ with ligand **5**. Selected ^{1}H-NMR assignments are indicated in the spectrum. Part A is the spectrum of the free DNA at 25 °C, and parts B and C correspond to the addition of 0.5 and 1.0 mole equiv of **5**, respectively, at 25 °C. Part D represents the spectrum of the 1:1 ligand **5**–DNA complex at 37 °C.

providing evidence for the binding to **5** to the decamer. When the temperature was raised to 37 °C, the ^{1}H-NMR signals of the 1:1 complex sharpened (see Figure 3D). Since the melting temperature of this decamer and its 1:1 complex with **3** under identical conditions were 47 and 76 °C, respectively (Lee et al., 1987), the DNA duplex would remain intact at 37 °C.

Assignments of the Nonexchangeable Protons and Characterization of the Binding of ***5*** *to d-[CATGGCCATG]$_2$.* The nonexchangeable ^{1}H-NMR signals of the 1:1 complex were assigned by using a combination of NOE difference, COSY, and NOESY methods (Lee et al., 1987, 1988). The COSY experiment of the 1:1 complex of **5** with d-[CATGGCCATG]$_2$ (data not shown) revealed one strong cytosine H5,H6, two weak CH5,H6 and two TH6,CH3 cross peaks in addition to those from the sugar protons. It has been reported that binding of a drug to or near a cytosine residue will lower the intensity of the CH5,H6 cross peak in the COSY spectrum (Borah et al., 1985), thus suggesting that compound **5** is located on C6 and C7. The reduction in the intensity of the CH5,H6 cross peaks is presumably due to the increase in the correlation times of cytosine residues upon binding with a drug.

In the NOESY spectrum of the 1:1 complex only CH5,H6, TH6,CH$_3$, and the base(H)-H2′/H2″ cross peaks were observed at mixing times of 0.1 and 0.4 s (data not shown). The NOE difference spectra of the 1:1 complex at 37 °C, using an irradiation time of 0.2 s, gave more informative results which are shown in Figure 4B–G, along with the reference spectrum (Figure 4A). Saturation of the low-field signal at 8.22 ppm (Figure 4B) gave NOEs at 7.73 ppm for CH6(1) and 1.38 ppm for a TCH$_3$ signal which was assigned to TCH$_3$-(3). Accordingly, the signal at 8.22 ppm was assigned to

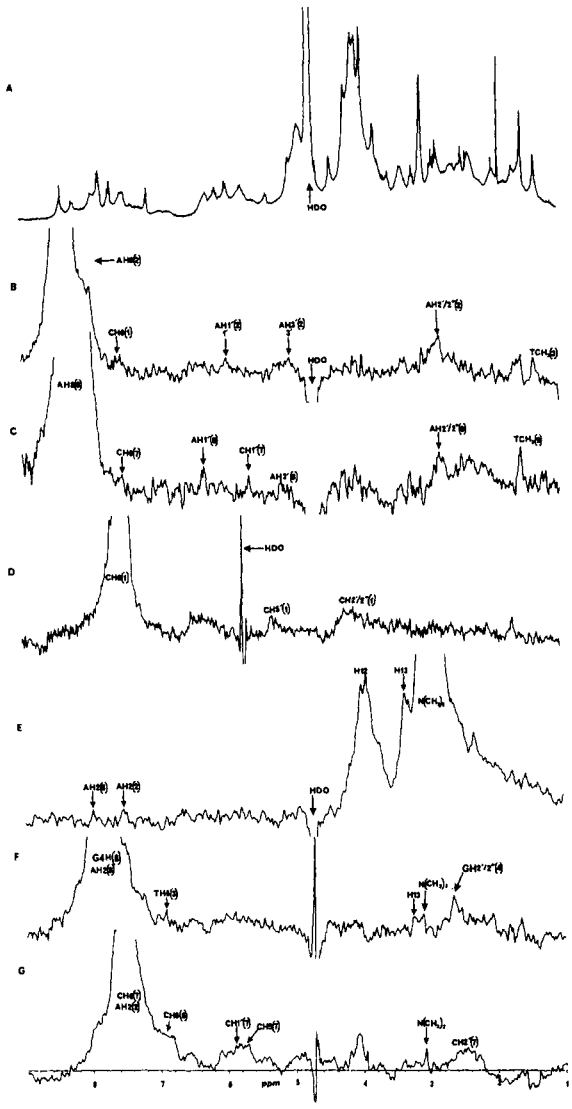

FIGURE 4: One-dimensional and NOE difference spectra of the 1:1 complex at 37 °C. Experimental conditions: irradiation time = 0.2 s, sweep width = 4000 Hz, pulse width = 17 μs, number of data points = 16 000, and 1024 FIDs were collected for each experiment. The arrows indicate the peaks that were saturated, and important NOEs are specifically denoted.

AH8(2), and other NOEs observed for AH2′/2″, AH3′, and AH1′ of A(2) were located at 2.5–3.0, 5.02, and 5.96 ppm, respectively, with relative intensity AH2′/2″ ≫ AH3′ ≥ AH1′, indicative of a conformation of the duplex that belongs to the B-family (Gronenborn & Clore, 1985). On the basis of COSY data, the signal at 7.13 ppm can then be ascribed to TH6(3). Therefore, the other TCH_3 signal at 1.58 ppm must belong to TCH_3(9), and the chemically exchanging resonances at 6.89 and 6.92 ppm can be assigned to TH6(9). Binding of a ligand to a self-complementary DNA oligomer destroys the dyad axis of the DNA and the two strands then give separate NMR resonances. The appearance of the chemically exchanging signals suggests that the association of **5** with the equivalent 5′-CCAT sites on d-[CATGGCCATG]$_2$ is slow on the NMR time scale. Saturation of the TH6(9) gave a NOE at 7.85 ppm for GH8(10). Saturation of the resonance at 8.08 ppm (Figure 4C) gave NOEs at ~7.50 ppm for a CH6 and at 1.58 ppm for a TCH_3 group, suggesting that these signals can be assigned to AH8(8), CH6(7), and TCH_3-(9), respectively. In addition, the relative NOE intensities of the sugar protons are in accordance with those expected for

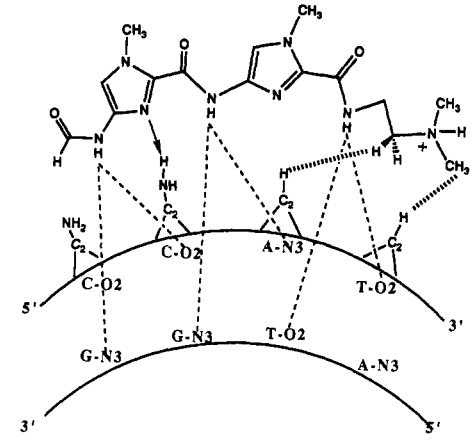

FIGURE 5: Depiction of molecular recognition components of ligand **5** on the 5′-CCAT sequence of the decadeoxyribonucleotide. Dotted lines represent hydrogen bonding between the amide NH groups on cytosine O2, guanine N3, adenine N3, and thymine O2. The thick arrow indicates the new hydrogen bond between G 2-NH_2 and the imidazole N3(N2). The NOEs observed between AH_2(2) and $-N(CH_3)_2$ and H13 of **5** and AH2(8) and $-N(CH_3)_2$ of **5** are denoted by the dashed lines.

the B-conformation. The conformation of the duplex in the 1:1 complex is similar to that of the free decamer (Lee et al., 1987), which suggests that binding of **5** to the DNA causes only minor distortions.

It is known that the H5′/5″ and H3′ signals at the 5′ and 3′ termini are the most shielded in their respective positions on the ^{1}H-NMR spectrum (Lown et al., 1985). Saturation of the CH6 signal at 7.73 ppm gave a NOE to the highest field H5′/5″ resonance at ~3.80 ppm (Figure 4D) and thus confirmed its assignment to CH6(1). Therefore the remaining chemically exchanging CH6 signals at 7.26 and 7.35 ppm must belong to CH6(6), and on the basis of the NOEs observed by irradiation of these signals, the peak at 7.80 ppm was assigned to GH8(5). Finally, the signal for GH8(4) at 7.75 ppm was assigned on the basis of the observed NOE with TH6(3) (Figure 4F).

From the nonselective inversion recovery experiments measured at 25 °C, a number of slowly relaxing signals were observed, and the chemically exchanging resonances at 7.54 and 7.56 ppm and the signal at 7.86 ppm were assigned to AH2(2,8) as will be discussed later (Kearns, 1984). Other slowly relaxing signals that belong to protons of **5** in the 1:1 complex were 8.22 (H1), 6.90 (H4,9), 3.80 (NCH_2C), 3.20 (CCH_2NMe_2), and 3.02 ppm [$-N(CH_3)_2$].

Location of **5** *on d-*$[CATGGCCATG]_2$. The ligand-induced chemical shift changes of the aromatic protons for each of the bases in the oligomer [$\Delta\delta$ (δ 1:1 complex – δ free DNA) 0, –0.23, –0.04, –0.10, +0.06, +0.14, +0.11, –0.31, –0.31, and –0.06 ppm for purine-H8, TH6, and CH5 of CATGGCCATG, respectively] showed that nucleotides C(6)–A(9) were most influenced by the binding of **5**. The location of **5** on this sequence was further corroborated by results from the NOE difference studies. Saturation of the $-N(CH_3)_2$ group at 3.02 ppm of **5** gave NOEs at ~7.54 and ~7.86 ppm indicative of its close proximity of AH2(2,8) (Figure 4E). Furthermore, saturation of the peak at 7.86 ppm (Figure 4F) gave NOEs to CCH_2NMe_2, and irradiation at 7.54 ppm (Figure 4G) produced a strong NOE to the $-N(CH_3)_2$ group of **5**. Accordingly the signals at 7.54 and 7.56 (exchanging signals) and 7.86 ppm were ascribed to AH2(2 and 8), respectively. These data illustrate that the ligand is bound in the minor groove of the C_6CAT_9 and the dimethylamino moiety at the

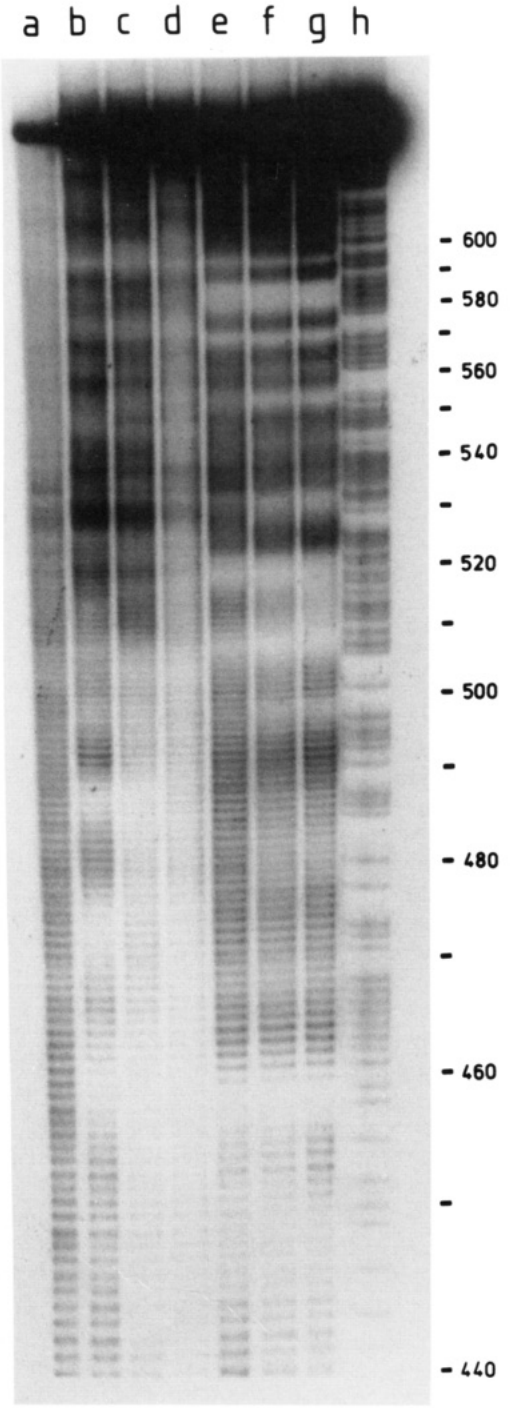

FIGURE 6: Autoradiogram of the MPE footprinting gel. Lane a, MPE; lanes b–d, **6**, 100, 250, and 500 μM, respectively; lanes e–g, **5**, 100, 250, and 500 μM, respectively; lane h, formic acid G,A lane.

C-terminus of **5** is oriented to T(9) while the imidazole moieties are situated in the GC region. This investigation also shows that the second methylene group on the C-terminus is in close proximity to AH2(2), and it is responsible for reading the 3′ AT site. This is consistent with previous reports (Lee et al., 1987, 1988), which showed that steric interactions between the methylene hydrogens and guanine 2-NH_2 moieties prevent the binding of the C-terminus to a GC site, thus forcing it to read an AT site. A model for the 1:1 complex of **5** and 5′-CCAT-3′ of the decamer is depicted in Figure 5.

MPE Footprinting. Compounds **4**–**7** were initially screened over a large dose range on a large fragment (*Hin*dIII/*Eco*RI) of pBR322 DNA (data not shown). The mono- and tetraimidazole analogues **4** and **7** gave poor footprints. The

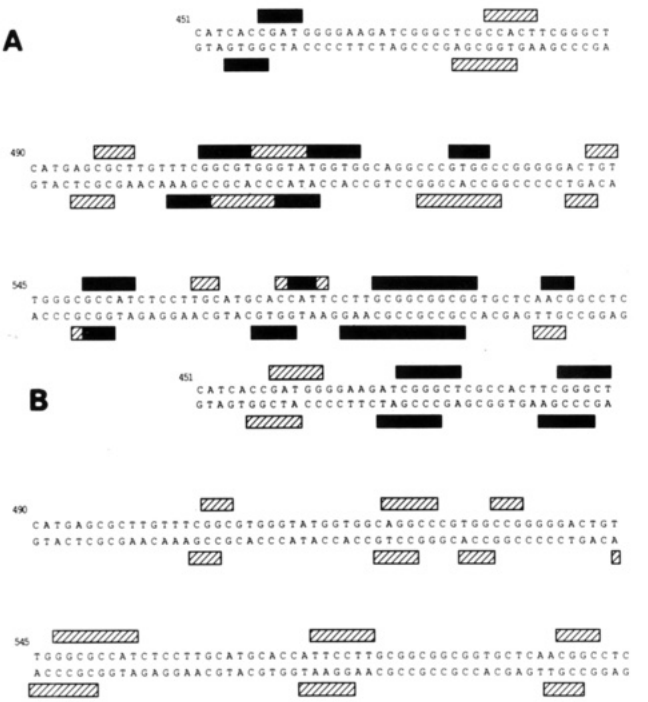

FIGURE 7: Densitometric analysis of the MPE footprinting autoradiograms on the *Bam*HI/*Sal*I fragment of pBR322 DNA. Solid and shaded boxes represent strong and weak footprint sites. Top boxes are for the *Bam*HI labeled DNA, and the bottom boxes are for the *Sal*I-labeled DNA. Parts A and B are for compounds **5** and **6**, respectively.

diimidazole **5** produced footprints identical to those of lexitropsin **3** which contains an amidinium group instead of a dimethylamino moiety (data not shown). The GC recognition of this compound was confirmed by densitometric analysis and in particular the binding of **5** to the sequence 5′-CCGT-3′. Compound **6** produced clear footprints, although at different sites from **5**.

In order to analyze in more detail the binding of **5** and **6**, a 275 base pair GC-rich fragment of pBR322 (*Bam*HI/*Sal*I) was isolated and data were obtained from both strands. A typical footprinting gel is shown in Figure 6. Distinct footprints are observed for both compounds and it is clear that they do not recognize the same sequences even though they differ only by one imidazole unit. These results clearly show that small changes in the molecules can produce significant changes in their sequence recognition.

Using electrophoresis runs of differing times it was possible to resolve an overlapping region of 150 base pairs from both strands. A detailed densitometric analysis was performed in this region and the data are summarized in Figure 7. Both the recognition of GC-rich sequences and the differences between the binding sites of **5** (Figure 7A) and **6** (Figure 7B) are clearly evident. For compound **5** a general preference for 5′-(G·C)$_3$(A·T) is observed, whereas the strongest sites for **6** are within two occurrences of the sequence 5′-TCGGGCT, which is not recognized by compound **5** (see Figure 7).

Molecular Modeling Studies. In order to follow the minor groove of DNA, the ligand must adopt a conformation isohelical to the DNA. Force field calculations predicted the minimum energy conformation of the imidazole analogues **4**–**7** in which the amide bonds are fixed in the s–Z conformations, a preference caused by stereoelectronic factors (Deslongchamps, 1983) which cannot be determined by such calculations. The MM2 energy-minimized conformations of **4**–**7** show that each molecule adopts a crescent-shaped

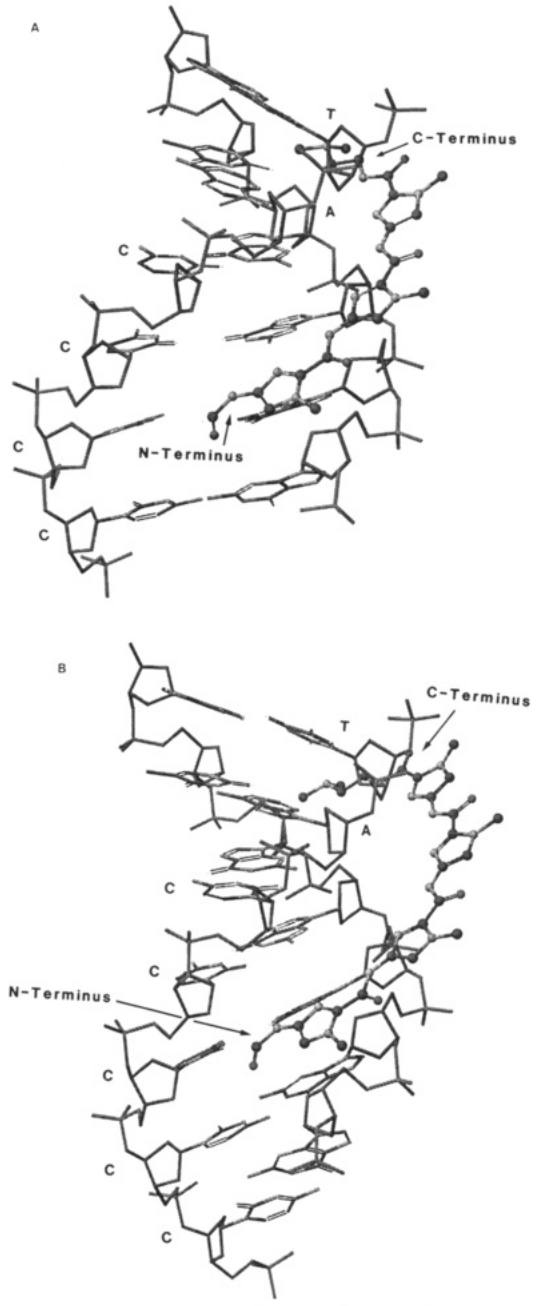

FIGURE 8: Energy-minimized conformers of the imidazole analogues **6** and **7** were docked into the minor groove of the underlined sequence of the B-oligonucleotides (part A) 5′-CCCCAT and (part B) 5′-CCCCCAT, respectively, with the dimethylamino moiety located over the T residue. The 1:1 complexes were not energy-minimized.

conformation which matches the convex surface of the minor groove of DNA. The planes of the imidazoles are coplanar and thus provide the necessary shape to fit snugly into the minor groove of the DNA and permit the amide protons and the imidazole N3 group to form hydrogen bonds with the electron-rich sites such as guanine N3, 2-NH_2, adenine N3, thymine O2 and cytosine O2.

The ideal distance of the helical axis to the amide hydrogen of the ligand which is isohelically bound to DNA can be estimated to be 4.5 Å. For an ideal B-DNA (h = 3.38 Å, t = 36°, π = 47.1°) with this radius (r = 4.5 Å), the repeating unit of the perfectly located ligand hydrogen, capable of forming hydrogen bonds, can be calculated to be 4.4 Å (Kumar et al., 1990; Goodsell & Dickerson, 1986). In the energy-minimized conformations of **4**–**7**, the distances between the amido NH groups lie between 4.5 and 4.9 Å, thus indicating that the formation of hydrogen bonds between consecutive base pairs and the ligand should be possible.

Further molecular modeling studies conducted in our laboratories included the consideration of the radius of curvature of the imidazole analogues. Cory et al. (1992) have shown that the curvature of netropsin and distamycin is 15 Å, which matches well with the curvature of the minor groove of AAAA (19 Å), thus explaining their strong isohelical binding to DNA. In our studies, the radius of curvature of the tetranucleotide d-[G_4·C_4], drawn in the B-conformation using the DNA/RNA builder program and displayed on the Tektronix CAChe system, was determined to be 19 ± 1 Å using the G 2-NH_2 groups as points on the circle. The curvatures of the energy-minimized conformations of **5**–**7** were measured to be 15, 17, and 13 ± 1 Å, respectively, using the carbon of the formyl moiety and the N-1 atom of the imidazoles. The increase in the curvature of the tetraimidazole analogue may explain the decrease in its binding constant to DNA.

In order to understand the implications of the increased curvature and reduced binding constant, the energy-minimized conformers of **4**–**7** were docked into the minor groove of the B-oligomers 5′-CCAT, 5′-CCCAT, 5′-CCCCAT, and 5′-CCCCCAT, respectively. In these complexes, the ligands are located on the underlined sequence with the dimethylamino group residing over the T residue as constrained from data obtained from the ^{1}H-NMR studies. The models, while not energy-minimized, show that analogue **6** fits snugly into the minor groove (see Figure 8A), and all the amido-NH groups can form bifurcated hydrogen bonds with the electron-rich sites (distances between the amido-N*H* groups and purine N3 and pyrimidine O2 are between 2.6 and 3.2 Å). However, due to the increase in the curvature of **7**, it is difficult to fit properly in the minor groove. If the terminal amido NH groups are positioned for hydrogen bonding with the electron-rich sites in the minor groove, then the central amido NH groups would be positioned too far (5–6 Å) for hydrogen bonding with the DNA (see Figure 8B) and thus destabilizes the ligand·DNA complex. This could explain the lower affinity to DNA by the tetraimidazole analogue **7** compared to the "shorter" triimidazole analogue.

These studies clearly show the length of three imidazole units is optimal for this class of compounds, and a further increase in the number of heterocycles to target for longer DNA sequences is not feasible due the "phasing" problem. Therefore, future developments of such imidazole-containing analogues of distamycin for long GC-rich sequences would have to include the use of linkers or develop heterocycles with smaller repeating units. The results of this work will be reported in due course.

ACKNOWLEDGMENT

The authors acknowledge the NSF-REU program and Research Corp. for support.

REFERENCES

Bains, W. (1989) *New Sci.* (May 6), 48–51.
Barton, J. K. (1986) *Science 232*, 727–734.
Borah, B., Roy, S., Zon, G., & Cohen, J. S. (1985) *Biochem. Biophys. Res. Commun. 133*, 380–388.
Burckhardt, G., Luck, G., Zimmer, C., Storl, J., Krowicki, K., & Lown, J. W. (1989) *Biochim. Biophys. Acta 1009*, 11–18.
Caruthers, M. H. (1980) *Acc. Chem. Res. 13*, 155–160.
Cory, M., Tidwell, R. R., & Fairlet, T. A. (1992) *J. Med. Chem. 35*, 431–438.

Debart, F., Periguad, C., Gosselin, D., Mrani, D., Rayner, B., Le Ber, P., Auclair, C., Balzarini, J., De Clercq, E., Paoletti, C., & Imbach, J.-L. (1989) *J. Med. Chem. 32*, 1074–1083.

Dervan, P. B. (1986) *Science 232*, 464–471.

Deslongchamps, P. (1983) *Stereoelectronic Effects in Organic Chemistry*, p 101, Pergamon, New York.

Frederick, C. A., Grable, J., Melia, M., Samudzi, C., JenJacobsen, L., Wang, B. C., Greene, P., Boyer, H. W., & Rosenberg, J. M. (1984) *Nature 309*, 327–331.

Goodsell, G., & Dickerson, R. E. (1986) *J. Med. Chem. 29*, 727–733.

Gronenborn, A. M., & Clore, G. M. (1985) *Prog. Nucl. Magn. Reson. Spectrosc. 17*, 1–32.

Gurskii, G. V., Tumanyan, V. G., Zasedatelev, A. S., Zhuze, A. L., Grokhovsky, S. L., & Gottikh, B. P. (1977) in *Nucleic Acid–Protein Recognition* (Vogel, H. J., Ed.) p 189, Academic Press, New York.

Hahn, F. E. (1975) in *Antibiotics III. Mechanisms of Action of Antimicrobial and Antitumor Agents* (Corcoran, J. W., & Hahn, F. E., Eds.) pp 79–100, Springer-Verlag, New York.

Hartley, J. A., Lown, J. W., Mattes, W. B., & Kohn, K. W. (1988) *Acta Oncol. 27*, 503–506.

Helene, C. (1990) *Chimicaoggi* (April), 65–67.

Hurley, L. H. (1989) *J. Med. Chem. 32*, 2027–2033.

Hurley, L. H., & Boyd, F. L. (1987) *Annu. Rep. Med. Chem. 22*, 259–268.

James, T. L. (1975) *Nuclear Magnetic Resonance in Biochemistry*, p 20, Academic Press, New York.

Kalk, A., & Berendsen, H. C. J. (1976) *J. Magn. Reson. 24*, 343–366.

Kearns, D. R. (1984) *CRC Crit. Rev. Biochem. 15*, 237–290.

Kissinger, K., Krowicki, K., Dabrowiak, J. C., & Lown, J. W. (1987) *Biochemistry 26*, 5590–5598.

Kopka, M. L., Yoon, C., Goodsell, D., Pjura, P., & Dickerson, R. E. (1985) *Proc. Natl. Acad. Sci. U.S.A. 82*, 1376–1380.

Krowicki, K., Lee, M., Hartley, J. A., Ward, B., Kissinger, K., Skorobogaty, A., Dabrowiak, J. C., & Lown, J. W. (1988) in *Structure and Expression* (Sarma, R. H., & Sarma, M. H., Eds.) Vol. 2, pp 251–271, Adenine Press, Guilderland, NY.

Kumar, S., Jaseja, M., Zimmerman, J., Yadagiri, B., Pon, R. T., Saspe, A.-M., & Lown, J. W. (1990) *J. Biomol. Struct. Dyn. 8*, 99–121.

Lee, M., Hartley, J. A., Pon, R. T., Krowicki, K., & Lown, J. W. (1987) *Nucleic Acids Res. 16*, 665–684.

Lee, M., Krowicki, K., Hartley, J. A., Pon, R. T., & Lown, J. W. (1988) *J. Am. Chem. Soc. 110*, 3641–3649.

Lown, J. W. (1982) *Acc. Chem. Res. 15*, 381–387.

Lown, J. W. (1988) *Anticancer Drug Des. 3*, 25–40.

Lown, J. W., Hanstock, C. C., Imbach, J. L., Rayner, B., & Vasseur, J. J. (1985) *J. Biomol. Struct. Dyn. 2*, 1125–1135.

Luck, G., Zimmer, C., Reinert, K. E., & Arcamone, F. (1977) *Nucleic Acids Res. 4*, 2655–2670.

Mack, D. P., Iverson, B. L., & Dervan, P. B. (1988) *J. Am. Chem. Soc. 110*, 7572–7574.

Mattes, W. B., Hartley, J. A., Kohn, K. W., & Matheson, D. W. (1988) *Carcinogenesis 9*, 2065–2072.

Morgan, A. R., Lee, J. S., Pulleyblank, D. F., Murray, N. L., & Evans, D. H. (1979) *Nucleic Acids Res. 7*, 547–569.

Ofengard, J. (1979) *Nature 282*, 449–450.

Rao, K. E., Zimmerman, J., & Lown, J. W. (1991) *J. Org. Chem. 56*, 786–797.

Takeda, Y., Ohlendorf, D. H., Anderson, W. F., & Matthews, B. W. (1983) *Science 221*, 1020–1026.

Taylor, J. S., Schultz, P. G., & Dervan, P. B. (1984) *Tetrahedron 40*, 457–465.

Thurston, D. E., & Thompson, A. S. (1990) *Chem. Br.* (August), 767–772.

Watson, J. D., Hopkins, N. H., Roberts, J. W., Steitz, J. A., & Weiner, A. M. (1987) in *Molecular Biology of the Gene* (4th Ed.), Benjamin/Cummings, Menlo Park, CA.

Younguist, R. S., & Dervan, P. B. (1985a) *Proc. Natl. Acad. Sci. U.S.A. 82*, 2565–2569.

Younguist, R. S., & Dervan, P. B. (1985b) *J. Am. Chem. Soc. 107*, 5528–5529.

Zakrzewska, K., Lavery, R., & Pullman, B. (1987) *J. Biomol. Struct. Dyn. 4*, 833–843.

Zimmer, C., & Wahnert, U. (1986) *Prog. Biophys. Mol. Biol. 47*, 31–112.

Zimmer, C., Luck, G., Burkhardt, G., Krowicki, K., & Lown, J. W. (1988) in *Structure and Expression* (Sarma, R. H., & Sarma, M. H., Eds.) Vol. 2, pp 291–303, Adenine Press, Guilderland, NY.